DYNAMICAL SIMULATION OF UNDERWATER SOUND PROPAGATION IN THE HORMOZ STRAIT

Z.Nour Ali Pour[1] , A.M. Arasteh[2] , M. Torabi Azad[3] ,Y. Bahman Pour [4]

1- Msc, Islamic Azad university, Tehran North Branch
2- Assistant Prof., Islamic Azad University, Tehran North Branch
3- Assistant Prof., Islamic Azad University, Tehran North Branch
4- Msc, Iran Telecommunication Research Center

Abstract

Providing an illustration of sound propagation in the Hormoz Strait ,this paper is about acoustic wave propagation in shallow water for a harmonic point source with low frequency, less than 1000 *Hz* and solution of a homogenous Helmholtz equation using parabolic equation. C++ programming is used to solve Helmholtz equation [9] and MATLAB software is used to illustrate figures and animate them [6], [7]. The input parameters are water characteristics such as, salinity, temperature, corresponding depth of the surface and of the bottom, in the software, as well as the number of frames. One can view animation of frames and see how salinity and temperature can effect on the sound propagation and how grazing angle come closer to the normal (vertical line) with respect to decrease of temperature and increase of salinity and depth in water column and therefore decrease of sound velocity, corresponding to Snell's law, increase of refraction index and specially at the Hormoz Strait. The convergence zone distances at the surface are more than two kilometres although it lowers at the bottom.

Keywords: Underwater Sound Propagation, Parabolic Equation, Hormoz Strait, Dynamical Simulation, Convergence Zone, Animation

1.Introduction

Historically, sonar technologists initiated the development of underwater acoustic modelling to improve sonar system design and evaluation efforts, principally in support of naval operations. Moreover, these models were used to train sonar operators, assess fleet requirements, predict sonar performance and develop new tactics [1].

Barkhatov (1968) and Zorning (1979) have presented detailed review of acoustic analog modelling. Pekeris (1984) used the normal-mode solution of the wave equation to explain the propagation of explosively generated sound of shallow water [4]. Harrison (1989), McCammon (1991), Buckingham (1992), porter (1993) and Dozier and Cavanagh (1993) have reviewed propagation modelling. Fast finite difference method has been used to accurately determine the real (versus imaginary) Eigen values (Porter and Resis, 1984). Lee and Pierce (1995) and Lee *et al.* (2000) carefully traced the historical development of the parabolic equation (PE) method in underwater acoustics. A two-way PE model (Collins and Evans, 1992) was developed to improve the computation of backscattered energy [1]. A.M. Arasteh *et al*. (2006) used C++ and MATLAB languages for simulation of underwater acoustics in Caspian sea and Persian gulf [9]. In this work, one could enter the speed of sound or SSP velocity and SSP depth as a point.

The purpose of this study was illustration of graphs with the effect of salinity, temperature, on the speed of sound in the underwater sound propagation.

This paper reports the progress on developing a computer code, which deals with numerical modelling of

[Downloaded from marine-eng.ir on 2026-11-04]
[DOR: 20.1001.1.17357608.1388.5.9.5.3]

acoustic wave propagation in the shallow water and the Hormoz Strait.

Shallow water, implies a dominant influence of the bottom on acoustic propagation paths because of scattering and reverberation, as well as physical constraints on submarine operations. Shallow water acoustics is distinctly different from the open ocean, which normally interacts quickly with both the sea surface and bottom, as seen in figures 9a, 9b, 9c, 9d and 9e. Numerous complications are experienced with the shallow water threat that one would not experience in deep water.

Possible effects of salinity on sound speed and bottom interaction on the propagation of sound are the two major changes in the shallow water environment. We ignored the second one because its data aren't available. Salinity can become a very important water column factor but pressure has the least effect on the speed of sound in seawater.

2.Theory

Acoustic wave equation

Acoustic wave propagation in an ocean medium for a harmonic point source is ruled by the reduced wave equation, a homogeneous Helmholtz equation

$$\nabla^2 P + k^2 P = 0 \qquad (1)$$

Where in Eq.(1) ∇^2 stands for Laplacian operator and P stands for $P(x,y,z)$, the wave field in Cartesian coordinates and $k = 2\pi f / C(x,y,z)$, the wave-number and f is source frequency and $C(x,y,z)$ is the sound- speed profile.

In Cylindrical coordinates, Eq(1) becomes:

$$\frac{\partial^2 P}{\partial r^2} + \frac{1}{r}\frac{\partial P}{\partial r} + \frac{\partial^2 P}{\partial z^2} + k_0^2 n^2(r,z)P = 0 \qquad (2)$$

Where $k = k_0 n$ and $k_0 = 2\pi f / C_0$, C_0 is a reference sound speed and $n(r,z) = C_0 / C(r,z)$ is the index of refraction.

We used the parabolic equation (PE) approximation method. Parabolic approximations to the reduced wave equation can be derived by a matrix that splits the total field into a transmitted field and a reflected field [5].

Let

$$k_1 = \frac{2\pi f}{C_1(r,z)} \qquad (3)$$

be the wave-number in medium 1, and

$$k_2 = \frac{2\pi f}{C_2(r,z)} \qquad (4)$$

be the wave-number in medium 2.

The partial differential equation representing the acoustic field on the interface is [4]:

$$u_{rr} + 2ik_0 u_r + \frac{\rho_1}{\rho_1+\rho_2}\left(k_2^2 + \frac{\rho_2}{\rho_1}k_1^2\right)u - k_0^2 u + \frac{2\rho_2}{h^2(\rho_1+\rho_2)}\left(u_{m-1} - \frac{\rho_1+\rho_2}{\rho_2}u_m + \frac{\rho_1}{\rho_2}u_{m+1}\right) = 0 \qquad (5)$$

We define the following two operators:

$$\tau_{zz}u = \frac{2\rho_2}{h^2(\rho_1+\rho_2)}\left(u_{m-1} - \frac{\rho_1+\rho_2}{\rho_2}u_m + \frac{\rho_1}{\rho_2}u_{m+1}\right) \qquad (6)$$

And

$$G = \frac{\rho_1}{\rho_1+\rho_2}\left(k_2^2 + \frac{\rho_2}{\rho_1}k_1^2\right) - k_0^2 + \tau_{zz} \qquad (7)$$

After substitution of (6) and (7) in (5), the result is the two-way far- field equation for the acoustic field with interface conditions.

[Downloaded from marine-eng.ir on 2026-11-04]
[DOR: 20.1001.1.17357608.1388.5.9.5.3]

The associated one-way outgoing wave equation is obtained by using the quadratic equation formula to formally solve Eq.(5) for $\frac{\partial u}{\partial r}$ as follows:

$$\frac{\partial u}{\partial r} = +i\left(\sqrt{k_0^2 + G} - k_0\right)u \tag{8}$$

For a range-independent medium, Eq.(8) is exact, that is, a solution of Eq.(8) is also a solution of Eq.(5). Using a rational function approximation for the square root operator and substituting into Eq.(8), one can Assume $\sqrt{k_0^2 + G}$ is constant over the interval $\left[r^n, r^{n+1}\right]$. Applying the Crank-Nicolson scheme to solve Eq.(8) and using definition (7) for G, simplifying then multiplying both sides by $k_0^2(\Delta z)^2(\rho_1+\rho_2)/2\rho_2$, regrouping terms gives

(9)

$$u_{m-1}^{n+1} + \left\{\left(\frac{W_1^*}{W_2^*}\right)\frac{k_0^2(\Delta z)^2(\rho_1+\rho_2)}{2\rho_2} - \frac{\rho_1+\rho_2}{\rho_2} + \frac{(\Delta z)^2 k_0^2}{2}\left[\frac{\rho_1}{\rho_2}(n_2^2-1)+(n_1^2-1)\right]\right\}u_m^{n+1} + \frac{\rho_1}{\rho_2}u_{m+1}^{n+1}$$

$$= \left(\frac{W_2}{W_2^*}\right)u_{m-1}^n + \left\{\left(\frac{W_1}{W_2^*}\right)\frac{k_0^2(\Delta z)^2(\rho_1+\rho_2)}{2\rho_2} - \left(\frac{W_2}{W_2^*}\right)\frac{(\rho_1+\rho_2)}{\rho_2} + \left(\frac{W_2}{W_2^*}\right)\frac{(\Delta z)^2 k_0^2}{2}\left[\frac{\rho_1}{\rho_2}(n_2^2-1)+(n_1^2-1)\right]\right\}u_m^n + \frac{\rho_1}{\rho_2}\left(\frac{W_2}{W_2^*}\right)u_{m+1}^n$$

Eq (9) may be expressed in matrix form as follows:

(10)

$$[(\nu_1,\nu_2,\nu_3)]\begin{bmatrix} u_{m-1}^{n+1} \\ u_m^{n+1} \\ u_{m+1}^{n+1}\end{bmatrix} = [(\hat{\nu}_1,\hat{\nu}_2,\hat{\nu}_3)]\begin{bmatrix} u_{m-1}^{n} \\ u_m^{n} \\ u_{m+1}^{n}\end{bmatrix}$$

Where

$$\nu_1 = 1 \tag{11}$$

(12)

$$\nu_2 = \left(\frac{W_1^*}{W_2^*}\right)\frac{k_0^2(\Delta z)^2(\rho_1+\rho_2)}{2\rho_2} - \frac{\rho_1+\rho_2}{\rho_2} + \left[\frac{(\Delta z)^2 k_0^2}{2}\frac{\rho_1}{\rho_2}(n_2^2-1)+(n_1^2-1)\right]$$

$$\nu_3 = \frac{\rho_1}{\rho_2} \tag{13}$$

$$\hat{\nu}_1 = \frac{W_2}{W_2^*} \tag{14}$$

(15)

$$\nu_2 = \left(\frac{W_1^*}{W_2^*}\right)\frac{k_0^2(\Delta z)^2(\rho_1+\rho_2)}{2\rho_2} - \left(\frac{W_2}{W_2^*}\right)\frac{(\rho_1+\rho_2)}{2} + \left(\frac{W_2}{W_2^*}\right)\left[\frac{(\Delta z)^2 k_0^2}{2}\frac{\rho_1}{\rho_2}(n_2^2-1)+(n_1^2-1)\right]$$

$$\hat{\nu}_3 = \frac{\rho_1}{\rho_2}\frac{W_2}{W_2^*} \tag{16}$$

Where the components ν_1, ν_2, ν_3, $\hat{\nu}_1$, $\hat{\nu}_2$ and $\hat{\nu}_3$ are defined by formulas (11)-(16)[2].

Our data of Hormoz Strait was collected during the oceanographic cruise ROPME sea area, summer 2001.

Data of 72nd station of Hormoz Strait with range of 10 kilometres is used. First, the graphs of animation with 5 frames with figures 1a to 1e are shown. Then different source frequencies from 100 *Hz* to 100 *KHz* are used at figures 2 to 9, with 1000 *Hz* source frequency, which can be observed frame by frame.

[Downloaded from marine-eng.ir on 2026-11-04]

[DOR: 20.1001.1.17357608.1388.5.9.5.3]

3.Results

Here, some of the results of simulation comprising a comparison between various source frequencies from 100 *Hz* to 100 *KHz* are presented.

Input parameters which can be entered by user, are water characteristics such as: Salinity, temperature and depth a 19/E as the number of frames, then the animation of graphs can be observed frame by frame from the surface to the bottom of water.

Figures 1a, 1b, 1c, 1d and 1e are 5 frames of 80th station of Hormoz Strait from one fifth of water characteristic, figure 1a, to the water characteristic of full depth, figure 1e, which is animated. At the first frame, salinity is minimum and temperature is maximum. At the last frame, salinity is maximum and temperature is minimum. If user selects 5 frames, one fifth of salinity is added to the minimum amount which is shown at the first graph and one fifth of temperature is decreased from the maximum at the first graph.

Description such as temperature, salinity, sound velocity and frequency, which is constant (here it is 1000 *Hz*) is written on them.

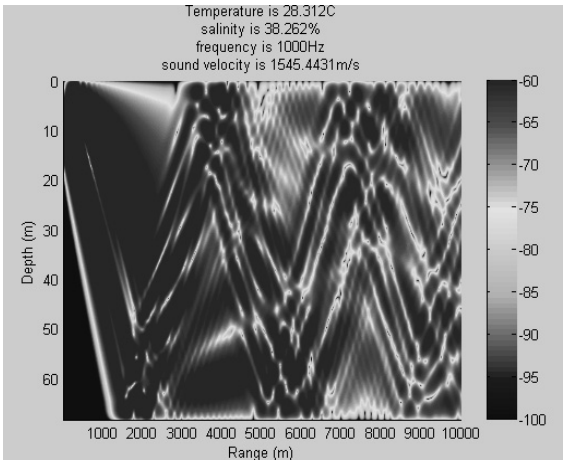


Fig.1a- The first figure of 80th station

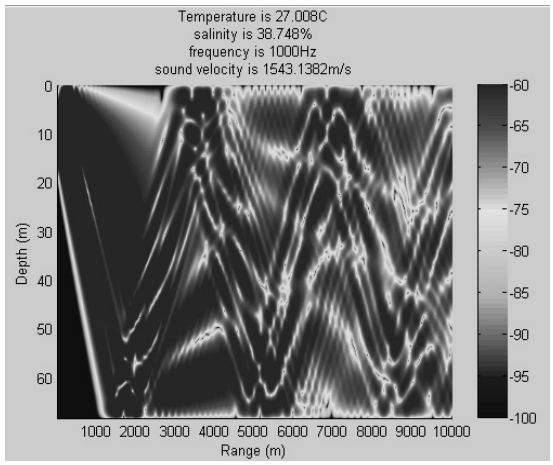


Fig.1b- The second figure of 80th station

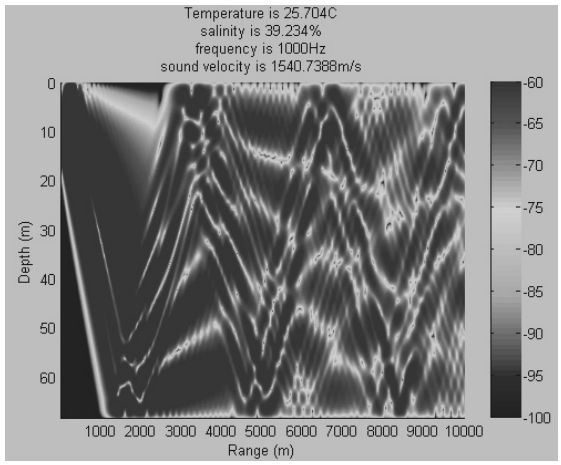


Fig.1c- The third figure of 80th station

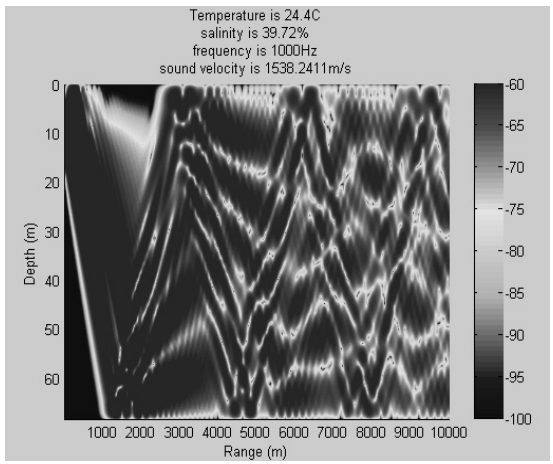


Fig.1d- The forth figure of 80th station

[Downloaded from marine-eng.ir on 2026-11-04]
[DOR: 20.1001.1.17357608.1388.5.9.5.3]

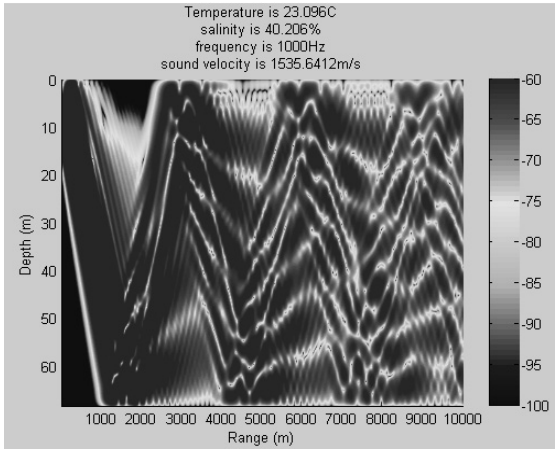


Fig.1e-The fifth figure of 80th station

Simulation results in a homogeneous represented using different source frequencies with final depth =76.82 m, source depth=5 m, final range=10000 m, ρ=1 gr/cm^3, temperature of surface=32.21 $^\circ C$, temperature of bottom=22.22 $^\circ C$, salinity of surface=37.55 psu, salinity of bottom =40.28 psu at the 72nd station of Hormoz Strait is shown at figures 2, 3, 4, 5, 6, 7, 8 and 9. As one see, parabolic equation is better for the frequencies less than 1000 Hz or low frequencies.

These animations start from figure 2 to 3 and 4 to 5 and 6 to 7 and 8 to 9. Temperature and salinity and frequency and sound velocity which are calculated with Medwin equation and contains six terms, are shown at each graph.

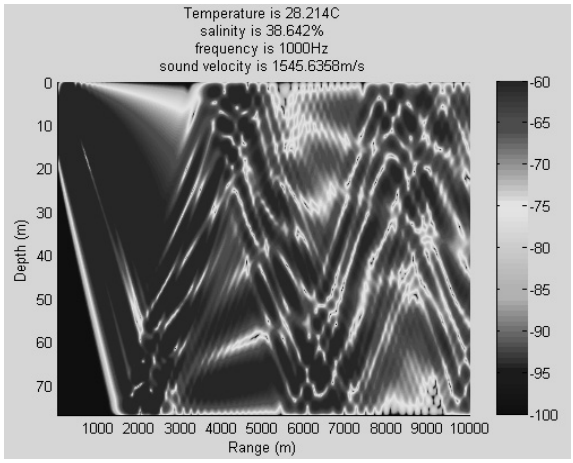


Fig. 2- First graph of 72nd station of Hormoz Strait with one fifth of water characteristics, source frequency is 1000 Hz .

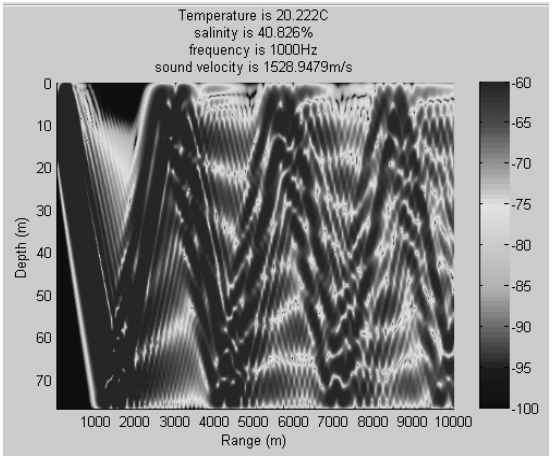


Fig.3- The fifth graph of 72nd station with water characteristic of full depth, source frequency is 1000 Hz .

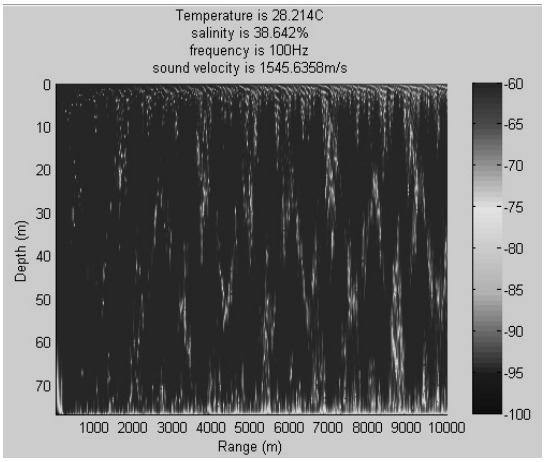


Fig.4- The first figure of 72nd station with one fifth of water characteristic, source frequency is 100 Hz .

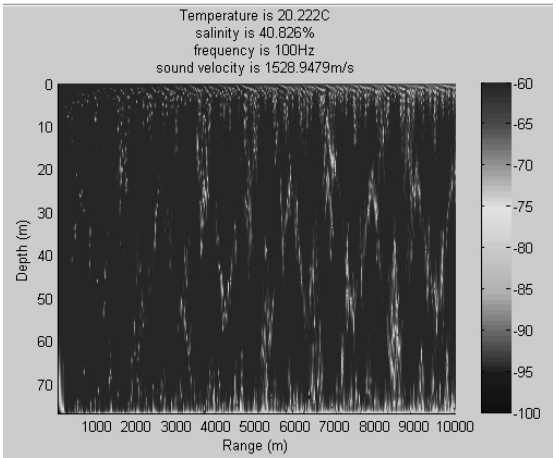


Fig.5- The fifth graph of 72nd station with water characteristic of full depth, source frequency is 100 Hz .

[Downloaded from marine-eng.ir on 2026-11-04]

[DOR: 20.1001.1.17357608.1388.5.9.5.3]

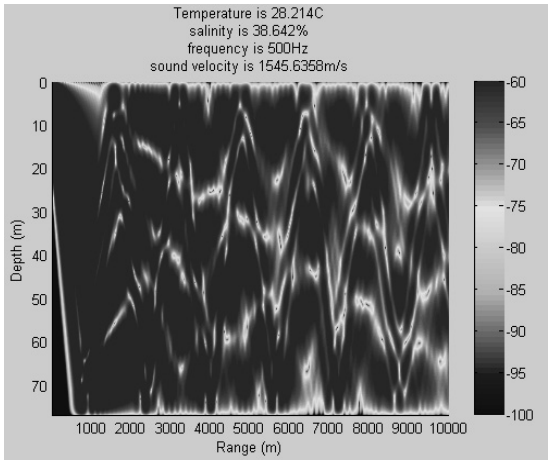


Fig.6- The first graph of 72nd station with one fifth of water characteristic, source frequency is 500 Hz .

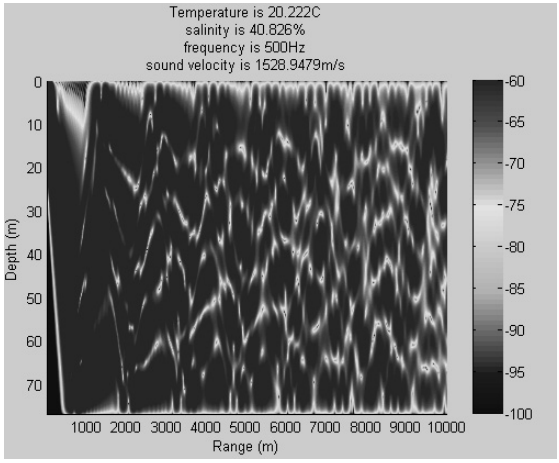


Fig. 7- The fifth graph of 72nd station with water characteristic full depth, source frequency is 500 Hz .

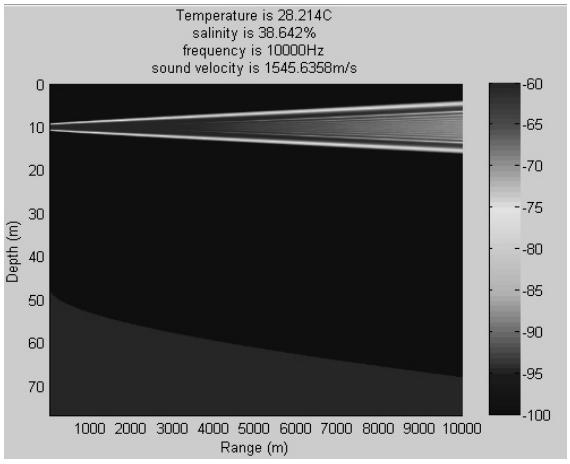


Fig.8- The first graph of 72nd station with one fifth of water characteristic, source frequency is 100000 Hz .

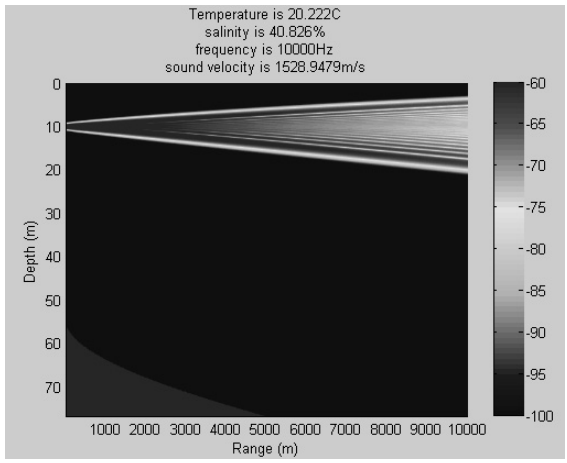


Fig.9- The last figure of 72nd station with water characteristic of full depth, source frequency is 100000 Hz .

According to both mathematical and physical complexities of problem, some of important parameters such as sediment and surface parameters are omitted.

Any change in salinity of one part per thousand will result changing of approximately 1.3 m/s in the sound speed. Pressure also causes a change in bulk modulus and density, and sound speed will increase 0.017 m/s for every meter of depth increase. This slight change is important where temperature remains constant. Temperature, the foremost factor affecting sound speed, usually decreases with depth, and this leads to an accompanying decrease in sound speed at the rate of approximately 3 m/s per degree Celsius. Below a depth of about 1,000 m, however, temperature is fairly constant, and the predominant factor affecting sound speed becomes pressure. When water with a negative speed gradient overlays a positive speed gradient, a sound channel is produced. Under these circumstances, any sound signal travelling in this area is refracted back and forth so that it becomes horizontally channeled. Sonar (Sound waves) originating with an initial upward inclination is refracted upward. Sonar from a sound source in this layer

[Downloaded from marine-eng.ir on 2026-11-04]
[DOR: 20.1001.1.17357608.1388.5.9.5.3]

that make a small angle with the horizontal are roughly sinusoidal, crossing and re-crossing the layer of minimum speed. This reinforcement of rays within the sound channel can continue until the sound is absorbed, scattered, or intercepted by some obstacle. Sounds travelling in this manner sometimes are received at extremely great distances from the source. These long ranges occur primarily as a result of two factors: absorption is small for a low-frequency sound and most of the sound energy from a sound source at the axis is confined to the channel.

It is obvious from Figures 1a… 1e that grazing angle from the surface to the bottom of water column comes closer to the normal (vertical line) and sound velocity is decreased from1545.4431 m/s at the surface to 1535.6412 m/s at the bottom, where temperature is reduced from 28.312 to 23.096 $^{\circ}C$ and salinity is increased from 39.95 to 41.23 psu. The convergence zone distances at one fifth of water characteristic such as salinity and temperature are about two kilometres although it lowers at full amount of them.

4. Discussion

One can observe how grazing angle comes closer to the normal (vertical line) and how the sound refracts with changes of salinity and temperature and their affect on sound propagation.

Ratio of index of refraction is:

$$\frac{n_2}{n_1} = \frac{C_1}{C_2} \qquad (17)$$

Where in Eq.(17) C_1, C_2 stand for speed of sound in media 1 and 2, respectively. The fundamental law which governs the refraction of sound is Snell's Law. It states that when sonar is transmitted into a new medium, the relationship between the angle of incidence and the angle of refraction is given by following equation (figure 10):

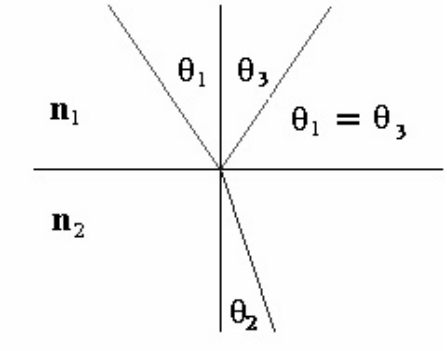


Fig.10- snell's law

$$n_1 \sin\theta_1 = n_2 \sin\theta_2 \qquad (18)$$

Where in Eq.(18) n_1, n_2 stand for the indexes of refraction of the incident and the refractive medium respectively and θ_1 and θ_2 are the angles between the normal (to the interface) plane and the incident waves, respectively.

If C_1 be assumed as sound velocity of media 1 and C_2 be assumed as sound velocity of media 2, then, considering equation (17), we will have $C_1 \rangle C_2$ and $n_2 \rangle n_1$, considering Eq.(18), $\sin\theta_1 \rangle \sin\theta_2$ and $\theta_1 \rangle \theta_2$, as they could be observed in all figures.

When all of the sound rays are returned back near the surface, they tend to converge into a small region. Therefore the sound pressure level is increased dramatically in this region known as a *convergence zones* (CZ), (figure 11).

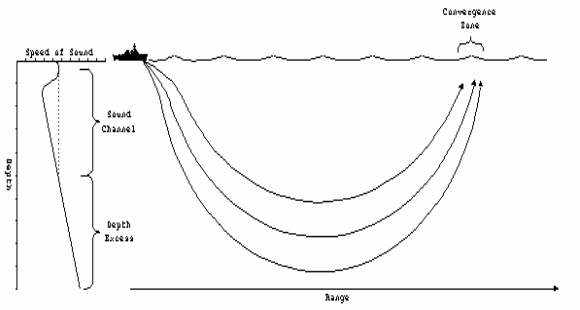


Fig.11- convergence zone

[Downloaded from marine-eng.ir on 2026-11-04]

[DOR: 20.1001.1.17357608.1388.5.9.5.3]

The CZ is only a few miles wide, and therefore, contacts which are acquired through convergence zones, tend to appear and disappear quickly. It may be possible for a ship to have a rather limited sonar range due to regular transmission losses but multiple convergence zones. These zones form protective rings about the ship. A hostile submarine closing in on the ship would be detected as it passes through the various convergence zones, thereby alerting the ship to its presence. The ship could then deploy mobile ASW assets like a helicopter to handle the submarine.

The simplest equation (Medwin, 1975) contains six terms, is used as follows:

$$C = 1449.2 + 4.6T - 0.055T^2 + 0.00029T^3 + (1.34 - 0.01T)(S - 35) + 0.016Z \quad (16)$$

Where in Eq.(16) C stands for the speed of sound in sea water (m/s), T is the water temperature $(^{\circ}C)$, S is the salinity ($^{\circ}/_{\circ\circ}$ or parts/1000 or psu) and Z is the depth of water (m) [8].

5. Conclusion

Animation of acoustic finite-difference codes is developed using c++ language for solving the Helmholtz equation and wave equation. MATLAB is used for illustrating graphs and making animation of them to model underwater acoustic propagation.

Formula and the method of parabolic equation for solving Helmholtz equation is presented. The underwater acoustics modelling shows affect of changes of salinity and temperature on sound propagation in Hormoz Strait and how grazing angle comes closer to the normal (vertical line) with respect to decrease of temperature and increase of salinity in water column. The convergence zone distances become lower when the depth increases.

6. References

1-Etter Paul C., (2003), Underwater acoustic modeling and simulation, 3rded, Spon Press, New York.

2-Lee D., and McDaniel S.T., (1987), Ocean acoustic propagation by finite difference methods: Naval Underwater Systems Center, pergamon press, New London, CT 06320, U.S.A.

3-Urick R.J, (1983), Principle of underwater sound, 3rd ed, McGraw-Hill book co., New York.

4-Lee D., and Schultz M.H,(1995), Numerical ocean acoustic propagation in three dimensions, World scientific.

5-McDaniel S.T. ,(1975), Propagation of normal mode in parabolic approximation, The Journal of the Acoustical Society of America ,Vol.57,Issue 2,PP.307- 311.

6-Eggen, C., and Howe, B., and Dushaw ,B. ,(2002),. A MATLAB GUI for ocean acoustic propagation. Ieee, 1(1), 1415-1421.

7-Mathworks, (2006), MATLAB function reference. Retrieved January 31, 2006. http://www.mathworks.com/access/helpdesk/help/techdoc/ref/refr.html

8-Dushaw, B., Worcester, P., Cornuelle, B., & Howe, B. , (1993), On equations for the speed of sound in seawater, Journal of the Acoustical Society of America, 93(1), 255-275.

9-Arasteh A. M. *et al*.,(2006), simulation of underwater sound propagation in Persian gulf and Caspian sea, , Islamic Azad university, Tehran North Branch, thesis of Msc (In Persian).

10-Nouralipour z. and Arasteh. A. M.,(2007), Kinds of modeling of underwater sound propagation and their differences, 7th conference on marine science and technology, noshahr (In Persian).

[Downloaded from marine-eng.ir on 2026-11-04]
[DOR: 20.1001.1.17357608.1388.5.9.5.3]